



UNIVERSITY OF LEEDS

This is a repository copy of *Marine anoxia and sedimentary mercury enrichments during the Late Cambrian SPICE event in northern Scotland*.

White Rose Research Online URL for this paper:
<http://eprints.whiterose.ac.uk/146235/>

Version: Accepted Version

Article:

Pruss, SB, Jones, DS, Fike, DA et al. (2 more authors) (2019) Marine anoxia and sedimentary mercury enrichments during the Late Cambrian SPICE event in northern Scotland. *Geology*, 47 (5). pp. 475-478. ISSN 1943-2682

<https://doi.org/10.1130/G45871.1>

© 2019 Geological Society of America. This is an author produced version of a paper published in *Geology*. Uploaded in accordance with the publisher's self-archiving policy.

Reuse

Items deposited in White Rose Research Online are protected by copyright, with all rights reserved unless indicated otherwise. They may be downloaded and/or printed for private study, or other acts as permitted by national copyright laws. The publisher or other rights holders may allow further reproduction and re-use of the full text version. This is indicated by the licence information on the White Rose Research Online record for the item.

Takedown

If you consider content in White Rose Research Online to be in breach of UK law, please notify us by emailing eprints@whiterose.ac.uk including the URL of the record and the reason for the withdrawal request.



eprints@whiterose.ac.uk
<https://eprints.whiterose.ac.uk/>

1 Marine anoxia and sedimentary mercury enrichments
2 during the Late Cambrian SPICE event in northern
3 Scotland

4 Sara B. Pruss¹, David S. Jones², David A. Fike³, Nicholas J. Tosca⁴, and Paul B.
5 Wignall⁵

6 ¹*Department of Geosciences, Smith College, Northampton, Massachusetts 01063, USA*

7 ²*Department of Geology, Amherst College, Amherst, Massachusetts 01002, USA*

8 ³*Department of Earth & Planetary Sciences, Washington University in St. Louis, St.
9 Louis, Missouri 63130, USA*

10 ⁴*Department of Earth Sciences, University of Oxford, Oxford OX1 3AN, UK*

11 ⁵*The School of Earth Sciences, Leeds University, Leeds, West Yorkshire LS2 9JT, UK*

12 **ABSTRACT**

13 Elevated mercury concentrations in ancient sedimentary rocks are used as a
14 fingerprint for large igneous province (LIP) volcanism because there is a tight association
15 between known LIPs and coeval sedimentary Hg anomalies. While **nonvolcanic**
16 processes of sedimentary Hg enrichment, including redox variations, have been
17 demonstrated in modern settings, interpretations of ancient sedimentary Hg records have
18 focused on LIP volcanism. Here, we document a link between sedimentary Hg
19 enrichment and marine redox changes **during** the **late** Cambrian Steptoean positive
20 isotopic carbon excursion (SPICE) event, a time with no known LIP. We report a new
21 occurrence of the SPICE event from the Eilean Dubh Formation of northern Scotland,
22 which preserves a series of coeval Hg enrichments. Abundant glauconite, a redox-

23 sensitive iron-bearing mineral, co-occurs stratigraphically with the SPICE and Hg
24 enrichments but is rare to absent from the rest of the section, and bioturbation is low in
25 strata spanning the SPICE. We suggest that local Hg enrichments were driven by
26 changing marine redox conditions during the SPICE event, rather than emplacement of a
27 LIP. Redox oscillations should be considered as an additional control on Hg enrichments
28 in the geologic record.

29 INTRODUCTION

30 Enrichments of Hg concentrations in ancient sedimentary rocks have been used as
31 a fingerprint of large igneous province (LIP) volcanism. All five major mass extinction
32 events and many Mesozoic **oceanic anoxic events** (OAEs) are linked to sedimentary Hg
33 anomalies; many are also synchronous with known LIP activity (e.g., Sanei et al., 2012;
34 Percival et al., 2015; Thibodeau et al., 2016). For some extinctions, a documented LIP
35 culprit is lacking, although Hg anomalies are observed (Jones et al., 2017; Racki et al.,
36 2018). While it is possible that in some cases the geologic record of massive volcanism is
37 not preserved, a broader suite of nonvolcanic processes may generate sedimentary Hg
38 enrichments (e.g., Shen et al., 2019; Them et al., 2019). Previous investigations of the
39 relationship between Hg (normalized to **total organic carbon** [TOC]) and redox
40 conditions during intervals of LIP volcanism yielded an equivocal or no relationship
41 between Hg/TOC and other redox proxies (Grasby et al., 2013; Percival et al., 2015);
42 however, those studies only examined the effect of Hg as it relates to TOC. Given that Hg
43 abundance can be tied to redox conditions and authigenic mineral formation in the
44 **present-day environment** (Emili et al., 2011), we provide a more systematic examination
45 of this proxy through the **late** Cambrian Steptoean positive isotopic carbon excursion

46 (SPICE) event. **[[Note: Informal divisions of the geologic time scale have been set**
47 **lowercase throughout, while formally defined periods are set in uppercase.]]**

48 Sedimentary Hg accumulation has been intensively studied in Holocene systems,
49 because Hg is toxic to animals and its methylated form, monomethylmercury (MeHg),
50 bioaccumulates in higher-order taxa (Morel et al., 1998). In laboratory experiments
51 designed to mimic marine anoxic events, Hg and MeHg were removed from the water
52 column and delivered to surface sediments by Fe and Mn oxyhydroxides, which scavenge
53 Hg under oxic conditions (Gagnon et al., 1997). Hg is, however, liberated from surface
54 sediments when oxygen is absent (Emili et al., 2011); bottom waters that have
55 experienced low-oxygen conditions have locally elevated Hg and MeHg concentrations
56 and can subsequently experience Hg drawdown through authigenic mineral formation
57 when oxygen is present again (Emili et al., 2011), thereby enriching the sedimentary Hg
58 inventory. These observations offer an interpretive framework for Hg cycling in the
59 geologic past. Here, we apply this framework to Upper Cambrian marine strata from
60 northern Scotland.

61 The Cambrian Period **was** characterized by large shifts in the carbon isotopic
62 record of carbonates (Maloof et al., 2005; Smith et al., 2015). Perhaps the most studied
63 Cambrian excursion is the SPICE, first recognized in western North America as a large
64 positive carbon isotope excursion in biologically depauperate carbonates of the Furongian
65 (late) Cambrian interval (Saltzman et al., 1998). This excursion also occurs globally in
66 Furongian strata (Glumac and Walker, 1998; Saltzman et al., 2000; Gill et al., 2011). In
67 Laurentia, the SPICE is found during an interval of coupled marine regression-
68 transgression (Saltzman et al., 2004), which has led some workers to propose that this

69 isotopic excursion **was** related to tectonic changes (Glumac and Walker, 1998) and
70 enhanced organic carbon burial (Saltzman et al., 2000). The extinction of trilobites
71 associated with the SPICE (Palmer, 1984) has been linked to low-oxygen conditions (Gill
72 et al., 2011) and/or warm ocean temperatures (Elrick et al., 2011). Sedimentological,
73 paleontological, and geochemical data all suggest significant, perhaps global,
74 environmental perturbation, although the ultimate cause of the carbon isotopic excursion
75 and redox changes is unclear.

76 **METHODS**

77 We collected samples at meter-scale **intervals** from rocks of the Upper Cambrian
78 Eilean Dubh Formation and Lower Ordovician Sailmhor Formation, northern Scotland.
79 Then, 1 to 2 g aliquots of powder were collected from each sample and analyzed for
80 $\delta^{13}\text{C}_{\text{carb}}$ and $\delta^{18}\text{O}_{\text{carb}}$ (**carb—carbonate**) using a Gas Bench II coupled to a Delta V
81 Advantage mass spectrometer at Washington University, **St. Louis, Missouri, USA**.
82 Results are reported in permil relative to the Vienna Peedee belemnite (VPDB) standard
83 in delta notation. Reproducibility of standards was 0.1‰ for $\delta^{18}\text{O}$ and 0.05‰ for $\delta^{13}\text{C}$.
84 Carbonate content of whole-rock powders was determined by mass loss following
85 dissolution with hydrochloric acid. Carbon content of insoluble residue was measured
86 with a Costech ECS 4010 elemental analyzer, with relative standard deviation of TOC
87 measurements <4.5%. Hg was measured on whole-rock powders with a Teledyne
88 Leeman Labs Hydra II_C mercury analyzer, with relative standard deviation <10%. TOC
89 and Hg analyses were done at Amherst College, **Amherst, Massachusetts**. Powder X-ray
90 diffraction was performed at Oxford University (UK) on hand-ground decarbonated
91 residues. Samples were mounted as a slurry mixed with anhydrous ethanol on a low-

92 background scattering silicon crystal substrate and analyzed using a Panalytical
93 Empyrean Series 2 diffractometer operating at 40 kV and 40 mA with a Co K α source.
94 Samples were analyzed while being continuously rotated, and data were acquired from 5°
95 to 85° 2 θ using a step size of 0.026°. Diffraction data were reduced using HighScore Plus
96 software, and mineral identification was based on correspondence to the International
97 Center for Diffraction Data Powder Diffraction File 4+ database
98 (<http://www.icdd.com/index.php/pdf-4/>). The amount and fractions of clay were
99 measured. Glauconite abundance in marine strata is a qualitative proxy for ancient
100 bottom-water oxygen levels, with high concentrations indicating redox oscillations (Tang
101 et al., 2017). We determined the abundance of glauconite in samples deposited **before**,
102 during, and after the SPICE event. We calculated the percent of glauconite from whole
103 rock using glauconite concentration in decarbonated residues and insoluble residue
104 concentration in the whole rock.

105 **RESULTS**

106 We identified a previously unrecognized manifestation of the SPICE event in the
107 Eilean Dubh Formation in northern Scotland, and we present accompanying Hg and
108 mineralogical data here (Fig. 1). The Eilean Dubh Formation lacks many useful
109 biostratigraphic fossils, but strata below it record the **Redlichiid-Olenellid extinction**
110 **carbon isotope excursion (ROECE)** and **Drumian carbon isotope excursion (DICE)** events
111 (Faggetter et al., 2018); the **Cambrian-Ordovician** boundary, defined by conodonts
112 (Huselbee and Thomas, 1998), occurs ~70 m above the Eilean Dubh excursion, placing
113 the excursion firmly within the Furongian. From a baseline value of ~-0.3‰, the onset of
114 the $\delta^{13}\text{C}$ excursion occurs at ~39.7 m above the base of the exposed section, reaches

115 values of 2.7‰, and returns to -1.0‰ at 70 m. Facies through this event lack
116 bioturbation and include stromatolitic and thrombolitic limestone and ribbon and
117 laminated limestone and dolostone. Below the SPICE, background Hg concentration is
118 ~1.0 ppb; the largest Hg enrichments begin at 42.9 m, with additional peaks through the
119 SPICE and up to 76.3 m (Fig. 1).

120 Because Hg is commonly bound to organic matter, we normalized Hg
121 concentration to TOC (Sanei et al., 2012) through the SPICE interval. Hg/TOC values are
122 elevated through the SPICE (Fig. 1). We excluded data with TOC \leq 0.006% (wt%; cf.
123 Grasby et al., 2016). TOC values range from 0.003% to 0.132% throughout the SPICE,
124 but they do not covary with Hg (Fig. 2; see also Fig. DR1 in the GSA Data Repository¹).
125 We used the mineralogical data to normalize Hg to clay abundance (Fig. 1; Fig. DR1).
126 Hg concentration has a stronger correlation with clay concentration than with TOC (Fig.
127 DR1), suggesting that Hg binding to clay minerals may be more important than to
128 organic matter in these rocks. Nonetheless, there is secular variability in the Hg/clay
129 ratio, with very low background Hg/clay values below and above the SPICE and enriched
130 Hg/clay values within the SPICE (Fig. 1). The occurrence of the Hg peaks within the
131 SPICE interval, regardless of the normalization used, strongly suggests a secular change
132 in Hg accumulation and burial during the SPICE.

133 **DISCUSSION**

134 **Mineralogical Constraints on Redox Conditions**

135 Various geochemical proxies have been developed to evaluate redox conditions in
136 ancient strata, including those based on trace-element abundance and isotopic
137 composition such as Cr, Fe, S, Mo, and U (Gill et al., 2011; Dahl et al., 2014; Planavsky

138 et al., 2014). A common technique used to reconstruct paleoredox conditions is the
139 reactive iron proxy, which measures ratios of highly reactive Fe (FeHR) to total iron
140 (FeT). Sediments deposited beneath oxic water can be distinguished from sediments
141 deposited under anoxic water columns based on their FeHR/FeT ratios (Raiswell and
142 Canfield, 1998). This proxy has been primarily applied to fine-grained siliciclastic
143 sediments, but because the SPICE in Scotland is hosted in strata with a mean carbonate
144 content of 90% (Table DR1), we developed an alternate mineralogical approach to
145 reconstructing redox conditions in the Eilean Dubh Formation.


146 The presence and/or abundance of authigenic minerals can constrain the redox
147 conditions of a particular depositional environment. For example, laboratory experiments
148 show that greenalite $[(\text{Fe}^{2+}, \text{Fe}^{3+})_{2-3}\text{Si}_2\text{O}_5(\text{OH})_4]$ forms in anoxic water columns,
149 providing constraints on the origin of iron formation (Tosca et al., 2016). More recently,
150 studies of fossils replaced by glauconite and/or apatite have linked these mineralogies to
151 redox oscillations (Pruss et al., 2017). Glauconite is an authigenic mixed-valence iron-
152 bearing phyllosilicate that forms in marine sediments under fluctuating redox conditions
153 (Odin and Létolle, 1980; O'Brien et al., 1990). Redox constraints on glauconite formation
154 have been well studied in modern systems (Odin and Létolle, 1980; O'Brien et al., 1990).
155 For example, glauconite is common in modern distal shelf deposits (Odin and Matter,
156 1981), where fluctuating local oxygen minimum zones drive the redox oscillations
157 necessary for glauconite formation. Strata deposited during the SPICE are enriched in
158 glauconite relative to underlying and overlying strata (Fig. 1). Glauconite is absent from
159 rocks below 37 m but makes up more than 2% (± 1.0 wt%) of the whole rock, and up to
160 20% of the noncarbonate fraction in many samples deposited during the SPICE.

161 Glauconite content generally remains far below 2% in strata above the SPICE, except for
162 sample 106.7.

163 A potential complication with utilizing glauconite abundances as a redox proxy is
164 that they can occur as either an authigenic or detrital component in rocks. While
165 glauconite requires oscillating redox conditions to form, its abundance may reflect
166 transport of allochthonous grains (Chafetz and Reid, 2000), in which case its presence
167 would not provide direct evidence for redox conditions at the site where it was ultimately
168 deposited. However, our lithostratigraphic data demonstrate that glauconite enrichment
169 occurred in shallow carbonate environments with minimal terrigenous input (Fig. DR1;
170 Table DR1). Moreover, while some detrital phases (e.g., quartz, K-feldspar) are present
171 in these rocks, they are neither more nor less abundant during the glauconite-bearing
172 SPICE interval (Table DR1; Fig. DR2). Whether the product of authigenic cement
173 formation or intrabasinal transport, we interpret the observed increase in glauconite in
174 strata spanning the SPICE as reflecting redox oscillations in the local marine environment
175 at the time of deposition; the sediments in which the glauconite formed **must** have
176 experienced low-oxygen conditions for at least some of their depositional history
177 (O'Brien et al., 1990). The absence of bioturbation in laminated limestone and dolostone
178 through the SPICE interval provides independent evidence for low oxygen, perhaps
179 periodically, through this part of the section. This inferred redox oscillation is consistent
180 with the redox control of Hg enrichments in sediments observed in laboratory
181 experiments and in Holocene environments (Emili et al., 2011). Taken together, we
182 interpret the Eilean Dubh SPICE event to have co-occurred with low-oxygen conditions

183 that oscillated with more oxic ones, allowing for glauconite formation and enhanced
184 sedimentary Hg accumulation.

185 **Local Manifestations of Global Trends in Anoxia?**

186 Multiple lines of independent evidence reported elsewhere suggest that the SPICE
187 broadly co-occurred with low-oxygen conditions [\[\[Cite relevant references here?\]\]](#) 

188 Nearly synchronous positive excursions in $\delta^{13}\text{C}$ and $\delta^{34}\text{S}$ and Mo depletion may reflect
189 the expansion of anoxic deeper waters (Gill et al., 2011), although anoxia may have been
190 time transgressive at basinal and global scales (Schiffbauer et al., 2017). The
191 heterogeneity of the sulfur isotopic record (Hurtgen et al., 2009; Gill et al., 2011),
192 interpreted to record changes in the global marine sulfate pool, points to low sulfate
193 concentrations in the global ocean, which may be linked to lower overall oxygen levels.

194 The U isotope record suggests a shift from oxic to transiently low-oxygen conditions
195 during the SPICE (Dahl et al., 2014), consistent with elevated pyrite and organic carbon
196 burial (Saltzman et al., 2011) and/or warmer ocean temperatures (Elrick et al., 2011).

197 The Hg proxy in marine sedimentary rocks may provide a way to track the local
198 redox changes in sedimentary successions. In the Eilean Dubh Formation, Hg abundance
199 increases (up to ~35 ppb) during the onset and throughout the SPICE but is low or absent
200 in the rest of the section. When controlled for TOC and clays, two sedimentary sinks for
201 Hg, these peaks remain. This suggests that the Hg proxy is sensitive to local redox
202 conditions, perhaps better constraining the timing of local anoxia than more global
203 proxies. Local expressions of anoxia are important to constrain, because the onset of
204 anoxia may be time transgressive within and/or between basins. In the Eilean Dubh
205 Formation, Hg abundance indicates an initial development of local low-oxygen

206 conditions at the onset of SPICE, with a peak in development during the falling limb of
207 the event. Here, it appears Hg abundance may track the onset and duration of low-oxygen
208 conditions, followed by a subsequent local oxygenation event; such patterns may be
209 useful for monitoring local redox conditions in other basins and at other times in geologic
210 history.

211 **CONCLUSIONS**

212 There is a strong and well-documented relationship between LIPs and
213 sedimentary Hg enrichment throughout the geologic record. However, our observations
214 for the SPICE in the Eilean Dubh Formation suggest that Hg enrichments do not
215 **necessarily** reflect excess Hg loading from a large volcanic source. Given the association
216 between Hg enrichment and glauconite formation, we argue for a redox control on Hg
217 accumulation during the SPICE in Scotland. Furthermore, many intervals for which LIPs
218 have been implicated in elevated Hg also co-occur with redox oscillations (Sanei et al.,
219 2012; Racki et al., 2018), underscoring the need to better understand the relationship
220 between Hg and redox.

221 **ACKNOWLEDGMENTS**

222 We acknowledge the assistance of M. Kopicki, L. Lim, H. Grotzinger, E.
223 Swislow, R. Chinitz, T. Browne, and K. Clayton in laboratory preparation and analysis of
224 samples. E. Roth provided field assistance, and L. Faggetter provided field and laboratory
225 assistance. Smith College and Amherst College are acknowledged for partial support of
226 this research. Acknowledgment is made to the Donors of the American Chemical Society
227 Petroleum Research Fund for partial support of this research (to Pruss).

228 **REFERENCES CITED**

- 229 Chafetz, H.S., and Reid, A., 2000, Syndepositional shallow-water precipitation of
230 glauconitic minerals: *Sedimentary Geology*, v. 136, p. 29–42,
231 [https://doi.org/10.1016/S0037-0738\(00\)00082-8](https://doi.org/10.1016/S0037-0738(00)00082-8).
- 232 Dahl, T.W., Boyle, R.A., Canfield, D.E., Connelly, J.N., Gill, B.C., Lenton, T.M., and
233 Bizzarro, M., 2014, Uranium isotopes distinguish two geochemically distinct stages
234 during the later Cambrian SPICE event: *Earth and Planetary Science Letters*, v. 401,
235 p. 313–326, <https://doi.org/10.1016/j.epsl.2014.05.043>.
- 236 Elrick, M., Rieboldt, S., Saltzman, M.R., and McKay, R.M., 2011, Oxygen-isotope trends
237 and seawater temperature changes across the late Cambrian Steptoean positive
238 carbon-isotope excursion (SPICE event): *Geology*, v. 39, p. 987–990,
239 <https://doi.org/10.1130/G32109.1>.
- 240 Emili, A., Koron, N., Covelli, S., Faganeli, J., Acquavita, A., Predonzani, S., and De
241 Vittor, C., 2011, Does anoxia affect mercury cycling at the sediment-water interface
242 in the Gulf of Trieste (northern Adriatic Sea)? Incubation experiments using benthic
243 flux chambers: *Applied Geochemistry*, v. 26, p. 194–204,
244 <https://doi.org/10.1016/j.apgeochem.2010.11.019>.
- 245 Faggetter, L.E., Wignall, P.B., Pruss, S.B., Sun, Y., Raine, R.J., Newton, R.J.,
246 Widdowson, M., Joachimski, M.M., and Smith, P.M., 2018, Sequence stratigraphy,
247 chemostratigraphy and facies analysis of Cambrian Series 2–Series 3 boundary strata
248 in northwestern Scotland: *Geological Magazine*, v. 155, p. 865–877,
249 <https://doi.org/10.1017/S0016756816000947>.

- 250 Gagnon, C., Pelletier, É., and Mucci, A., 1997, Behaviour of anthropogenic mercury in
251 coastal marine sediments: *Marine Chemistry*, v. 59, p. 159–176,
252 [https://doi.org/10.1016/S0304-4203\(97\)00071-6](https://doi.org/10.1016/S0304-4203(97)00071-6).
- 253 Gill, B.C., Lyons, T.W., Young, S.A., Kump, L.R., Knoll, A.H., and Saltzman, M.R.,
254 2011, Geochemical evidence for widespread euxinia in the later Cambrian ocean:
255 *Nature*, v. 469, p. 80–83, <https://doi.org/10.1038/nature09700>.
- 256 Glumac, B., and Walker, K.R., 1998, A late Cambrian positive carbon-isotope excursion
257 in the Southern Appalachians: Relation to biostratigraphy, sequence stratigraphy,
258 environments of deposition, and diagenesis: *Journal of Sedimentary Research*, v. 68,
259 p. 1212–1222, <https://doi.org/10.2110/jsr.68.1212>.
- 260 Grasby, S.E., Sanei, H., Beauchamp, B., and Chen, Z., 2013, Mercury deposition through
261 the Permo–Triassic biotic crisis: *Chemical Geology*, v. 351, p. 209–216,
262 <https://doi.org/10.1016/j.chemgeo.2013.05.022>.
- 263 Grasby, S.E., Beauchamp, B., and Bond, D., 2016, Mercury anomalies associated with
264 three extinction events (Capitanian crisis, latest Permian extinction and the
265 Smithian/Spathian extinction) in NW Pangea: *Geological Magazine*, v. 153, p. 285–
266 297, <https://doi.org/10.1017/S0016756815000436>.
- 267 Hurtgen, M.T., Pruss, S.B., and Knoll, A.H., 2009, Evaluating the relationship between
268 the carbon and sulfur cycles in the later Cambrian ocean: An example from the Port
269 au Port Group, western Newfoundland, Canada: *Earth and Planetary Science Letters*,
270 v. 281, p. 288–297, <https://doi.org/10.1016/j.epsl.2009.02.033>.

- 271 Huselbee, M.Y., and Thomas, A.T., 1998, *Olenellus* and conodonts from the Durness
272 Group, NW Scotland, and the correlation of the Durness succession: *Scottish Journal*
273 *of Geology*, v. 34, p. 83–88, <https://doi.org/10.1144/sjg34010083>.
- 274 Jones, D.S., Martini, A.M., Fike, D.A., and Kaiho, K., 2017, A volcanic trigger for the
275 Late Ordovician mass extinction? Hg data from South China and Laurentia:
276 *Geology*, v. 45, p. 631–634, <https://doi.org/10.1130/G38940.1>.
- 277 Maloof, A.C., Schrag, D.P., Crowley, J.L., and Bowring, S.A., 2005, An expanded record
278 of early Cambrian carbon cycling from the Anti-Atlas margin, Morocco: *Canadian*
279 *Journal of Earth Sciences*, v. 42, p. 2195–2216, <https://doi.org/10.1139/e05-062>.
- 280 Morel, F.M.M., Kraepiel, A.M.L., and Amyot, M., 1998, The chemical cycle and
281 bioaccumulation of mercury: *Annual Review of Ecology and Systematics*, v. 29,
282 p. 543–566, <https://doi.org/10.1146/annurev.ecolsys.29.1.543>.
- 283 O'Brien, G.W., Milnes, A.R., Veeh, H.H., Heggie, D.T., Riggs, S.R., Cullen, D.J.,
284 Marshall, J.F., and Cook, P.J., 1990, Sedimentation dynamics and redox iron-
285 cycling: Controlling factors for the apatite-glaucinite association on the East
286 Australian continental margin, *in* Notholt, A.J.G., and Jarvis, I., eds., *Phosphorite*
287 *Research and Development*: Geological Society [London] Special Publication 52,
288 p. 61–86, <https://doi.org/10.1144/GSL.SP.1990.052.01.06>.
- 289 Odin, G.S., and Létolle, R., 1980, Glaucinitization and phosphatization environments: A
290 tentative comparison, *in* Bendor, Y.K., ed., *Marine Phosphorites*: Society of
291 Economic Paleontologists and Mineralogists (SEPM) Special Publication 29, p. 227–
292 237.

- 293 Odin, G.S., and Matter, A., 1981, De glauconiarum origine: *Sedimentology*, v. 28,
294 p. 611–641, <https://doi.org/10.1111/j.1365-3091.1981.tb01925.x>.
- 295 Palmer, A.R., 1984, The biomere problem: Evolution of an idea: *Journal of Paleontology*,
296 v. 58, p. 599–611, [https://doi.org/10.2307/1304904?refreqid=search-](https://doi.org/10.2307/1304904?refreqid=search-gateway:4b0209cceeccada3bdd9f059fc28852e)
297 [gateway:4b0209cceeccada3bdd9f059fc28852e](https://doi.org/10.2307/1304904?refreqid=search-gateway:4b0209cceeccada3bdd9f059fc28852e).
- 298 Percival, L.M.E., Witt, M.L.I., Mather, T.A., Hermoso, M., Jenkyns, H.C., Hesselbo,
299 S.P., Al-Suwaidi, A.H., Storm, M.S., Xu, W., and Ruhl, M., 2015, Globally
300 enhanced mercury deposition during the end-Pliensbachian extinction and Toarcian
301 OAE: A link to the Karoo-Ferrar large igneous province: *Earth and Planetary*
302 *Science Letters*, v. 428, p. 267–280, <https://doi.org/10.1016/j.epsl.2015.06.064>.
- 303 Planavsky, N.J., Reinhard, C.T., Wang, X., Thomson, D., McGoldrick, P., Rainbird,
304 R.H., Johnson, T., Fischer, W.W., and Lyons, T.W., 2014, Low Mid-Proterozoic
305 atmospheric oxygen levels and the delayed rise of animals: *Science*, v. 346, p. 635–
306 638, <https://doi.org/10.1126/science.1258410>.
- 307 Pruss, S.B., Dwyer, C.H., Smith, E.F., Macdonald, F.A., and Tosca, N.J., 2017,
308 Phosphatized early Cambrian archaeocyaths and small shelly fossils (SSFs) of
309 southwestern Mongolia: *Palaeogeography, Palaeoclimatology, Palaeoecology*,
310 v. 513, p. 166–177, <https://doi.org/10.1016/j.palaeo.2017.07.002>.
- 311 Racki, G., Rakociński, M., Marynowski, L., and Wignall, P.B., 2018, Mercury
312 enrichments and the Frasnian-Famennian biotic crisis: A volcanic trigger proved?:
313 *Geology*, v. 46, p. 543–546, <https://doi.org/10.1130/G40233.1>.

- 314 Raine, R.J., 2009, The Durness Group of NW Scotland: A Stratigraphical and
315 Sedimentological Study of a Cambro-Ordovician Passive Margin Succession [Ph.D.
316 thesis]: Birmingham, UK, University of Birmingham, 270 p.
- 317 Raiswell, R., and Canfield, D.E., 1998, Sources of iron for pyrite formation in marine
318 sediments: *American Journal of Science*, v. 298, p. 219–245,
319 <https://doi.org/10.2475/ajs.298.3.219>.
- 320 Saltzman, M.R., Runnegar, B., and Lohmann, K.C., 1998, Carbon isotope stratigraphy of
321 Upper Cambrian (Steptoean Stage) sequences of the eastern Great Basin: Record of a
322 global oceanographic event: *Geological Society of America Bulletin*, v. 110, p. 285–
323 297, [https://doi.org/10.1130/0016-7606\(1998\)110<0285:CISOUC>2.3.CO;2](https://doi.org/10.1130/0016-7606(1998)110<0285:CISOUC>2.3.CO;2).
- 324 Saltzman, M.R., Ripperdan, R.L., Brasier, M., Lohmann, K., Robison, R., Chang, W.,
325 Peng, S., Ergaliev, E., and Runnegar, B., 2000, A global carbon isotope excursion
326 (SPICE) during the late Cambrian: Relation to trilobite extinctions, organic-matter
327 burial and sea level: *Palaeogeography, Palaeoclimatology, Palaeoecology*, v. 162,
328 p. 211–223, [https://doi.org/10.1016/S0031-0182\(00\)00128-0](https://doi.org/10.1016/S0031-0182(00)00128-0).
- 329 Saltzman, M.R., Cowan, C.A., Runkel, A.C., Runnegar, B., Stewart, M.C., and Palmer,
330 A.R., 2004, The late Cambrian SPICE ($\delta^{13}\text{C}$) event and the Sauk II-Sauk III
331 regression: New evidence from Laurentian basins in Utah, Iowa and Newfoundland:
332 *Journal of Sedimentary Research*, v. 74, p. 366–377,
333 <https://doi.org/10.1306/120203740366>.
- 334 Saltzman, M.R., Young, S.A., Kump, L.R., Gill, B.C., Lyons, T.W., and Runnegar, B.,
335 2011, Pulse of atmospheric oxygen during the late Cambrian: *Proceedings of the*

- 336 National Academy of Sciences of the United States of America, v. 108, p. 3876–
337 3881, <https://doi.org/10.1073/pnas.1011836108>.
- 338 Sanei, H., Grasby, S.E., and Beauchamp, B., 2012, Latest Permian mercury anomalies:
339 Geology, v. 40, p. 63–66, <https://doi.org/10.1130/G32596.1>.
- 340 Schiffbauer, J.D., Huntley, J.W., and Fike, D.A., 2017, Decoupling biogeochemical
341 records, extinction, and environmental change during the Cambrian SPICE event:
342 Science Advances, v. 3, p. 1–7, <https://doi.org/10.1126/sciadv.1602158>.
- 343 Shen, J., Algeo, T.J., Chen, J., Planavsky, N.J., Feng, Q., Yu, J., and Liu, J., 2019,
344 Mercury in marine Ordovician/Silurian boundary sections of South China is sulfide-
345 hosted and non-volcanic in origin: Earth and Planetary Science Letters, v. 511,
346 p. 130–140, <https://doi.org/10.1016/j.epsl.2019.01.028>.
- 347 Smith, E.F., Macdonald, F.A., Petach, T.A., Bold, U., and Schrag, D.P., 2015, Integrated
348 stratigraphic, geochemical, and paleontological late Ediacaran to early Cambrian
349 records from southwestern Mongolia: Geological Society of America Bulletin,
350 v. 128, p. 442–468, <https://doi.org/10.1130/B31248.1>.
- 351 Tang, D., Shi, X., Ma, J., Jiang, G., Zhou, X., and Shi, Q., 2017, Formation of shallow-
352 water glaucony in weakly oxygenated Precambrian ocean: An example from the
353 Mesoproterozoic Tieling Formation in North China: Precambrian Research, v. 294,
354 p. 214–229, <https://doi.org/10.1016/j.precamres.2017.03.026>.
- 355 Them, T.R., II, Jagoe, C.H., Caruthers, A.H., Gill, B.C., Grasby, S.E., Gröcke, D.R., Yin,
356 R., and Owens, J.D., 2019, Terrestrial sources as the primary delivery mechanism of
357 mercury to the oceans across the Toarcian oceanic anoxic event (Early Jurassic):

358 Earth and Planetary Science Letters, v. 507, p. 62–72,

359 <https://doi.org/10.1016/j.epsl.2018.11.029>.

360 Thibodeau, A.M., Ritterbush, K., Yager, J.A., West, A.J., Ibarra, Y., Bottjer, D.J.,

361 Berelson, W.M., Bergquist, B.A., and Corsetti, F.A., 2016, Mercury anomalies and

362 the timing of biotic recovery following the end-Triassic mass extinction: Nature

363 Communications, v. 7, p. 11147, <https://doi.org/10.1038/ncomms11147>.

364 Tosca, N.J., Guggenheim, S., and Pufahl, P.K., 2016, An authigenic origin for

365 Precambrian greenalite: Implications for iron formation and the chemistry of ancient

366 seawater: Geological Society of America Bulletin, v. 128, p. 511–530,

367 <https://doi.org/10.1130/B31339.1>.

368 **FIGURE CAPTIONS**

369 Figure 1. Map showing measured section near Durness, Scotland (modified from Raine,

370 2009). Base of section is 58°37'35.33"N, 4°47'50.90"W. All data are presented in Table

371 DR1 (see footnote 1).

372

373 Figure 2. Stratigraphic column of Upper Cambrian upper Eilean Dubh Formation

374 measured at Balnakeil Bay in northern Scotland, with accompanying geochemical data:

375 carbon isotopes (VPDB [Vienna Peedee belemnite]), Hg abundance (ppb), Hg/TOC

376 (TOC—total organic carbon; ppb/wt%), Hg/clay (ppb/wt%), and glauconite abundance

377 (wt% relative to whole rock [WR]) are shown.

378

379 ¹GSA Data Repository item 2019xxx, [\[\[Please provide DR title\(s\) and brief](#)

380 [descriptions here.\]\]](#), is available online at

Publisher: GSA
Journal: GEOL: Geology
DOI:10.1130/G45871.1

381 <http://www.geosociety.org/datarepository/2019/>, or on request from

382 editing@geosociety.org.